Molecular Genetics and Metabolism Reports 34 (2023) 100956

Contents lists available at ScienceDirect

Molecular Genetics and Metabolism Reports

journal homepage: www.elsevier.com/locate/ymgmr

Non-invasive intravenous administration of AAV9 transducing iduronate sulfatase leads to global metabolic correction and prevention of neurologic deficits in a mouse model of Hunter syndrome

Kanut Laoharawee [a], Kelly M. Podetz-Pedersen [a], Tam T. Nguyen [a], Sajya M. Singh [a], Miles C. Smith [a], Lalitha R. Belur [a], Walter C. Low [b], Karen F. Kozarsky [c,1], R. Scott McIvor [a,*]

[a] Center for Genome Engineering, Department of Genetics Cell Biology and Development, 6-160 Jackson Hall, 321 Church St. SE, Minneapolis, MN 55455, USA
[b] Department of Neurosurgery; University of Minnesota, Minneapolis, USA
[c] REGENXBIO Inc., Rockville, MD, USA

ARTICLE INFO

Keywords:
Hunter syndrome
Metabolic disorder
Mucopolysaccharidosis type II
Gene therapy
Gene transfer
MPS II

ABSTRACT

Hunter syndrome is a rare x-linked recessive genetic disorder that affects lysosomal metabolism due to deficiency of iduronate-2-sulfatase (IDS), with subsequent accumulation of glycosaminoglycans heparan and dermatan sulfates (GAG). Enzyme replacement therapy is the only FDA-approved remedy and is an expensive life-time treatment that alleviates some symptoms of the disease without neurocognitive benefit. We previously reported successful treatment in a mouse model of mucopolysaccharidosis type II (MPS II) using adeno-associated viral vector serotype 9 encoding human IDS (AAV9.hIDS) via intracerebroventricular injection. As a less invasive and more straightforward procedure, here we report intravenously administered AAV9.hIDS in a mouse model of MPS II. In animals administered 1.5×10^{12} vg of AAV9.hIDS at 2 months of age, we observed supraphysiological levels of IDS enzyme activity in the circulation (up to 9100-fold higher than wild-type), in the tested peripheral organs (up to 560-fold higher than wild-type), but only 4% to 50% of wild type levels in the CNS. GAG levels were normalized on both sides of the blood-brain-barrier (BBB) in most of tissues tested. Despite low levels of the IDS observed in the CNS, this treatment prevented neurocognitive decline as shown by testing in the Barnes maze and by fear conditioning. This study demonstrates that a single dose of IV-administered AAV9.hIDS may be an effective and non-invasive procedure to treat MPS II that benefits both sides of the BBB, with implications for potential use of IV-administered AAV9 for other neuronopathic lysosomal diseases.

1. Introduction

Mucopolysaccharidosis type II (MPS II, Hunter syndrome) is a rare X-linked recessive inherited lysosomal storage disorder (LSD) [1]. The disease is caused by mutations in the *iduronate-2-sulfatase* (*IDS*) gene, leading to defective or deficient iduronate-2-sulfatase (IDS) enzyme. IDS is the first step in the metabolic pathway for breakdown of glycosaminoglycans heparan and dermatan sulfates, which are normally processed in the lysosome. IDS removes O-linked sulfate moieties from the terminal iduronide, allowing the polymer to be further processed. Deficient IDS enzyme leads to aberrant accumulation of glycosaminoglycans in the lysosome, causing inflammation and cell death. The disease spectrum ranges from attenuated to severe, the latter exhibiting skeletal dysplasia, short stature, hepatosplenomegaly, cardiovascular disease, deafness, and neurocognitive deficits. MPS II disease manifestations can go unnoticed, becoming apparent around 6 months of age [2]. Most affected individuals succumb to the disease within the first two decades of life [3]. To date, enzyme replacement therapy (ERT; Elaprase) is the only FDA approved treatment for MPS II. ERT involves once- or twice- a week 8-h intravenous infusions into the patient. Despite the high cost [4] and frequency of ERT, it is considered a life-long treatment that slows the progression of disease and alleviates some symptoms but without neurocognitive benefit [5]. IDS modified for transit across the BBB via the transferrin receptor [6] has shown some neurologic benefit in clinical trials [7]. Allogenic hematopoietic stem cell transplantation (HSCT) is not generally practiced for MPS II due to early reports of neurologic

* Corresponding author.
E-mail address: mcivo001@umn.edu (R.S. McIvor).
[1] Current affiliation: SwanBio Therapeutics, Bala Cynwyd, Pennsylvania.

https://doi.org/10.1016/j.ymgmr.2023.100956
Received 13 January 2023; Accepted 13 January 2023

ineffectiveness [8]. Although more recent studies have reported neurocognitive improvement in MPS II patients when transplanted <2 years of age [9–11], HSCT is nonetheless associated with significant morbidity and mortality especially in the absence of a matched sibling donor. These circumstances prompt research for new and effective therapeutic approaches to address the limitations of currently available treatments.

Recently there have been significant advances in both clinical and preclinical development of genetic therapies for MPS II. One approach is transplantation of autologous hematopoietic stem cells (HSC) that have been stably transduced with an IDS-encoding lentiviral vector (LV), thereby providing much improved levels of IDS expression compared to allotransplant while eliminating the risk of graft-vs-host disease [12]. Several groups have reported high levels of IDS expression as well as treatment effectiveness in addressing metabolic, skeletal and neurologic manifestations of disease in MPS II mice engrafted with IDS-LV transduced HSC [12–15]. Several groups have also reported the effectiveness of AAV-mediated gene transfer for both metabolic and neurologic outcomes in MPS II mice [16–18]. AAV9-mediated IDS gene transfer has subsequently been initiated in clinical trials by REGENXBIO whereby the vector is delivered into the cisterna magna or intracerebroventricularly for direct access through the cerebrospinal fluid to the CNS [19]. AAV8 has also been used as a delivery vehicle for zinc-finger nuclease mediated homologous insertion of the IDS coding sequence downstream of the albumin promoter in the livers of MPS II mice. The animals showed systemic metabolic correction and the treatment prevented the emergence of neurologic deficits [20].

The ultimate goal of effective MPS treatment is not only for metabolic correction but also to address neurocognitive deficits. In preclinical studies AAV vectors have been delivered directly to the CNS in mice to achieve effective neurologic outcomes in several MPS studies, including MPS II [21–26]. We reported high levels of IDS expression systemically and correction of GAG storage in the brain as well as prevention of neurocognitive deficit after intracerebroventricular infusion of AAV9 encoding human IDS in MPS II mice [17]. Given the transduction versatility of AAV9 and its reported effectiveness in crossing the BBB, we reasoned that a less invasive systemic route of administration can be considered.

Intravenous administration (IV) of AAV9 has shown broad distribution on both sides of the BBB in several preclinical studies [21,27–31]. This means that IV-administration of AAV9 could potentially be an effective and non-invasive procedure to achieve neurologic benefit for MPS disease. Here we report that a single dose of IV administered AAV9.hIDS in the mouse model of MPS II resulted in stable and high-level IDS enzyme activity in the circulation and in peripheral organs. We also observed a range of 4–50% wt IDS enzyme activity in the CNS at 22-weeks post treatment. These levels of IDS enzyme led to global normalization of GAGs on both sides of the BBB and prevention of neurocognitive decline in the IV-treated MPS II mice. The results suggest that IV administration of AAV9.hIDS could potentially be used as a non-invasive and an effective gene therapy that benefits organs and cells on both sides of the BBB for MPS II. Finally, this study implicates the use of IV AAV9 administration for treatment of other diseases associated with neurologic deficit.

2. Materials and methods

2.1. rAAV9.hIDS viral vector

The IDS expression cassette with CB.7 regulating human IDS (hIDS) was constructed, packaged into rAAV9 and purified at Penn Vector Core (Philadelphia, PA), and provided by REGENXBIO Inc. (Rockville, MD) as previously described [17].

2.2. Animal care and husbandry

All animal care and experimental procedures were conducted with approval of the Institutional Animal Care and use Committee (IACUC) of the University of Minnesota. C57BL/6 iduronate-2-sulphatase knockout (*IDS* KO) mice were kindly provided by Dr. Joseph Muenzer (University of North Carolina, NC) and maintained under pathogen-free conditions at Research Animal Resources (RAR) facilities of the University of Minnesota. MPS II male pups ($IDS^{-/0}$) were generated by breeding heterozygous ($IDS^{+/-}$) C57BL/6 females to wild type ($IDS^{+/0}$) C57BL/6 males. All pups were genotyped by PCR.

2.3. Recombinant AAV9 (rAAV9) vector administration

At eight weeks of age, mice were briefly restrained and infused with a single dose of 1.51×10^{12} vector copies (vg) rAAV9 vector via intravenous injection through a lateral tail vein.

2.4. In-life sample collection

Blood was collected periodically throughout the study via submandibular puncture using sterile 5 mm lancets (Goldenrod) into microvette heparinized tubes and centrifuged in an Eppendorf centrifuge 5415D at 7000 rpm for 10 min. Plasma was collected and stored at −20 °C to −80 °C for IDS assay. Urine was collected periodically and stored at −20 °C until assay for GAG (Accurate Chemical, NY) and creatinine assay (Sigma-Aldrich, MO).

2.5. Tissue harvest and processing

At the end of study, animals were humanely euthanized using a CO_2 fume chamber at a rate of 2 L/min for 3 min, then perfused by hand pressure with 60 mL of 1× phosphate-buffered saline (PBS) in a 60 mL syringe with a SURFLO winged infusion set size 23Gx¾ (Terumo, NJ). The heart, lung, liver, spleen, kidney, and spinal cord were harvested and immediately snap frozen and stored at −80 °C. The brain was microdissected into 12 regions: left and right hemispheres of cerebellum, cortex, hippocampus, striatum, olfactory bulb, and thalamus/brainstem, and immediately snap frozen and stored at −80 °C.

Organs were processed using a Bullet blender STORM bead mill homogenizer (Next Advance) as previously described [20]. In brief, organs were cut into small pieces and transferred into preassigned 1.5 mL locked-cap tubes containing 200–400 μL of sterilized saline solution. The tubes were placed in the Bullet blender for homogenization at speed 12 for 5 min. Tissue homogenates were transferred into new GeneMate 1.5 mL microtubes (VWR, PA) and stored at −20 °C for qPCR. The remaining tissue homogenates were centrifuged at 13,000 rpm for 15 min at 4 °C. The entire supernatant was then transferred into a new 1.5 mL microtube and stored at −20 °C to −80 °C for IDS, GAG, and protein assay.

2.6. Iduronate sulfatase assay

4-methylumbelliferyl-α-L-iduronide-2-sulfate disodium (4-MU-aIdoA-2S, Toronto Research Chemical Incorporation; Cat. #M334715) was used as substrate for a two-step IDS enzymatic assay as previously described [24]. In brief, for the first-step reaction, plasma or tissue lysate was mixed with the substrate and incubated at 37 °C for 90 min. PiCi buffer was added into the reaction tube to stop the first-step reaction. Ten μL of 5 μg/mL Iduronidase (IDUA; Cat. #4119-GH-010, R&D Systems, MN) was immediately added to start the second-step reaction, and then incubating overnight at 37 °C. Stop buffer (0.5 M Na_2CO_3 + 0.5 M $NaHCO_3$, 0.025% Triton X-100, pH 10.7) was added into the reaction tube to terminate the second-step reaction. The reaction tube was then centrifuged at 13,000 rpm for 1 min, and the supernatant containing 4-MU (product of the reaction) was transferred into a round-bottom black 96-well plate. The plate was read at excitation 365 nm, and emission 450 nm, 75 sensitivity using a Synergy MX plate reader and spectrophotometer (Bio Tek, VT) with Gen5 program. Enzyme activity is

reported in nmol/h/ml for plasma and in nmol/h/mg protein for tissue lysates. Protein was assessed using Pierce 660 nm Protein Assay Reagent with bovine serum albumin as standard (Cat. #22662 and 23,208, respectively; Thermo Scientific, MA).

2.7. Glycosaminoglycan assay (GAG assay)

Tissue lysate was treated overnight with Proteinase K, DNase 1 and RNase, as previously described [25]. GAG content was measured by mixing treated tissue lysate using the Blyscan Sulfated Glycosaminoglycan Assay kit according to the manufacturer's protocol (Cat. #CLRB1000; Accurate Chemical, NY) with Blyscan glycosaminoglycan standard 100 μg/mL (Cat. #CLRB1010; Accurate Chemical, NY). The reaction was measured at 656 nm using a Synergy MX plate reader and spectrophotometer (Bio Tek, VT) with Gen5 program. Blank values were subtracted from all readouts. GAG content is reported in μg/mg protein for tissue lysates and μg/mg creatinine for urine samples. Urine creatinine was assessed using Creatinine Assay Kit (Cat. #MAK080 Sigma-Aldrich, MO).

2.8. Quantitative PCR (qPCR) for rAAV9 vector

Tissue homogenate was mixed with lysis buffer (5Prime) and proteinase K, gently rocking overnight at 55 °C. DNA was isolated using a phenol/chloroform extraction protocol. For qPCR, 60 ng of DNA template was mixed with 10 μL of FastStart Taqman Probe Master mix (Roche, Switzerland), 200 nmol each of forward and reverse primers, and 100 nmol of Probe36, (Cat. #04687949001); Roche). The reaction mix was placed into a C1000 Touch Thermo cycler (Bio-Rad, CA) with CFX manager software v3.1 for the qPCR reaction as previously described [17]. IDS forward primers: 5'-TCCCTTACCTCGACCCTTTT; and IDS reverse primer: 5'-CACAAGGTCCATGGATTGC. Vector copy was calculated and reported as vector genomes per cellular genome equivalent (vg/ge).

2.9. Neurocognitive tests

Barnes Maze is a measure of spatial navigation and learning memory, as previously described [32]. It is comprised of a 4-ft diameter circular platform containing 40 holes spaced equally around the perimeter at a height of 4 ft from the floor. All of the holes are blocked except one hole, which is open to the escape box. Different visual cues are attached to each of the 4 walls for spatial navigation. The ceiling of the room is equipped with a bright light and a camera to record the mouse. At 4 months post treatment, each test mouse was placed (one mouse at a time) in the middle of the platform with an opaque funnel covering the mouse. The funnel was lifted, and the mouse was given 3 min to find the escape hole. Each mouse was tested in 4 trials a day for a total period of 6 days. The latency to escape was recorded for each trial and the average was calculated for each day in each group.

Fear conditioning is used to assess learning memory of a fear response (i.e. the length of freezing time) to a conditioned stimulus (the environmental cues that associate with aversive experiences) as previously described [33]. A semi-automated video-monitoring fear-conditioning apparatus with Med Associates software was used to collect and analyze the data. The test is comprised of 3 sections over a course of two consecutive days: conditioning (training day; day 1), contextual fear testing (day 2), and cued fear testing (day 2). For conditioning, the test chamber was sprayed with Simple Green solution as an olfactory cue, and the mice were exposed to five pairings; a 60-s intertrial interval of cue presentation consists of 80-dB white noise and light (15 s) that co-terminated with a mild foot shock (0.7 mA, 1 s). Twenty-four hours later, contextual fear was assessed; the chamber was sprayed with Simple Green, the mice were placed in the chamber for 3 min without either cues (sound and light) or foot shock to assess freezing response (fear) associated with aversive contextual environment. The mice were rested for at least 2 h, followed by the cue fear test; the mice were placed in the chamber with altered contextual elements (i.e. floor, wall and odor) for 3 min without cues or foot shock to assess a nonspecific freezing behavior as a baseline, and immediately followed by an exposure of a 3-min light and sound (without foot shock) to assess the fear (freezing) associated to aversive cues.

2.10. Statistical analyses

Data are reported as mean +/− standard error (SE). Statistical analyses were performed using Prism 6. Two-way analysis of variance with Tukey's post-test was used to evaluate the significance of differences among test groups for IDS assay, GAG assay, and neurobehavioral assay, with a p-value of <0.05 considered significant. Treatment x time (learning slope) interaction was determined by ANOVA as described by Inman-Wood et al. [34]

3. Results

3.1. High levels of plasma and tissue IDS after intravenous administration of rAAV9.hIDS in MPS II mice

To determine the effectiveness of intravenously administered rAAV9.hIDS in MPS II mice, animals at 6 to 8-week of ages were divided into 3 groups of 10 mice each: rAAV9.hIDS-treated MPS II mice, untreated MPS II mice, and untreated normal male littermates. MPS II mice in the treatment group received rAAV9.hIDS at a dose of 1.51×10^{12} vg per mouse via the lateral tail-vein at 8 weeks of age. IDS enzymatic activity was subsequently assayed every 2–4 weeks to determine the overall level of rAAV9.hIDS transduction and expression of the therapeutic IDS transgene. Plasma was collected periodically for 22 weeks post injection. Consistent with our previous ICV study [24], IDS activity was undetectable in the plasma of the untreated MPS II littermates (Fig. 1), while low levels of IDS activity were observed in the plasma of the wild-type littermates (<60 nmol/h/mL). In stark contrast, remarkably increased levels of plasma IDS activity were observed in the treated MPS II group and maintained throughout the 22-week course of study. Increased plasma IDS activity was observed as early as 4-weeks post vector administration (week 4 mean = 274,000 nmol/h/mL) and maintained well above 77,500 nmol/h/mL for at least 22 weeks post treatment (Fig. 1; $p < 0.0001$) The levels of plasma IDS activity ranged from around 1300- to 9100-fold higher than those of the wild-type group. These data demonstrate that a single IV administration of rAAV9.hIDS

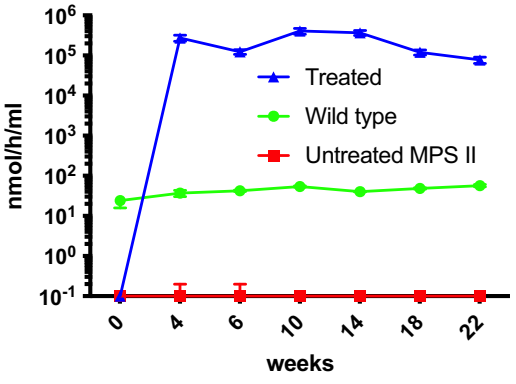

Fig. 1. Plasma IDS activity. IDS activities in the plasma of wild-type, untreated MPS II, and IV-rAAV9.hIDS treated animals were measured over the course of the 22-week study. IDS activity was undetectable in the plasma of untreated MPS II littermates (red). IV-injection of rAAV9.hIDS vector resulted in significantly increased and sustainable levels of IDS activity in the plasma of treated animals when compared to wild-type levels (****$p < 0.0001$). IDS activities in the rAAV-hIDS treatment group were elevated from 1300- to 9100-fold compared to wild-type.

vector leads to stable supraphysiological expression and secretion of IDS into the circulation.

To further investigate the effect of IV-administered rAAV9.hIDS, peripheral organs (heart, lung, liver, spleen and kidney) were harvested postmortem at the end of the 22-week study. Animals were perfused and cleared tissue homogenates were prepared to measure IDS activities. Some background fluorescence in the IDS assay (<0.1 nmol/h/mg protein) was observed in the heart, lung, liver, spleen and kidney of the untreated MPS II control group (Fig. 2A), while IDS activities of the wild-type control group were observed in the heart, lung, liver, spleen and kidney at 3.75, 134.2, 16.5, 53.4 and 18.2 nmol/h/mg protein, respectively. In contrast to the untreated MPS II group, the IV-treated group showed remarkably increased levels of IDS activity in the heart, lung, liver, spleen and kidney at 2175, 268, 5602, 1184, 406 mean nmol/h/mg protein, respectively. These tissue IDS activities of the treated mice surpassed the wild-type levels of IDS by 560-, 1.2-, 226-, 20- and 16-fold, respectively. These results demonstrate that IV administration of rAAV9.hIDS leads to high levels of IDS activities in the tested peripheral organs of the treated MPS II mice.

The major challenge of ERT and HSCT for Hunter syndrome is the lack of IDS enzyme penetration to the CNS through the BBB. We further investigated whether IV-administration of rAAV9.hIDS would lead to accumulation of IDS enzyme in the CNS. The brain was collected and microdissected into a total of 12 regions: the left and the right hippocampus, cortex, striatum, thalamus/brainstem, olfactory bulb, cerebellum, and the spinal cord. These CNS samples were processed, and tissue lysates assayed for IDS activity. The assay background showed little to no tissue IDS activity (<1.7 nmol/h/mg protein) in the 12 portions from untreated MPS II mice (Fig. 2B). As we have previously reported, IDS activities in brain tissue samples from wild-type littermates were much higher (up to 325 nmol/h/mg protein in R hippocampus) than in peripheral tissues (Fig. 2A). Surprisingly, IV-administration of rAAV9.hIDS resulted in low but detectable IDS activities in all of the 12 portions of the brain, ranging from 12 nmol/h/mg protein in right hippocampus to 43 nmol/h/mg protein in right olfactory bulb, (Fig. 2B). These levels of IDS activity in the different portions of the brain ranged between 4 and 51% of the observed wildtype IDS levels. These results demonstrate that a single IV administration of rAAV9.hIDS leads to low but corrective (see below) levels of IDS activity in the CNS.

3.2. qPCR confirms global transduction of rAAV9.hIDS vector in IV-administered MPS II mice

To confirm that IV-administration leads to global transduction of the viral vector, DNA was isolated from tissue homogenates for qPCR to determine vector distribution in peripheral organs and the CNS (Fig. 3). While a strikingly high vector copy number was found in the liver (286 vg/cell genome equivalent), much lower copy numbers were observed in the heart, lung, spleen and kidney (Fig. 3A, 4.7, 3.2, 1.9, and 2.7 vg/ge, respectively). Unlike the peripheral organs, relatively low vector copy numbers were observed in the 12 portions of the brain and the spinal cord (Fig. 3B, <0.6 vg/ge) of the IV-treated mice. Nonetheless these data demonstrate that IV-administration of rAAV9-hIDS leads to global transduction of the cells on both sides of the BBB.

3.3. IV administration of rAAV9.hIDS leads to global correction of glycosaminoglycans

One of the clinical symptoms in MPS II patients is elevated GAG levels in the urine, which also manifests in the mouse model of MPS II [35]. To determine the effect of IV rAAV9-hIDS treatment on GAG metabolism, urine was collected from all experimental animals at 10-, 14-, 18-, and 22-weeks post infusion. IV administration of rAAV9.hIDS into MPS II mice resulted in normalization of GAG levels in the urine by week 10 and throughout the time course of 22-week study. In contrast, GAG levels in urine of the untreated mice remained significantly higher than that of the treated animals and the wild-type littermates (Fig. 4A; $p < 0.05$).

One of the ultimate goals of the treatment is global reduction of GAGs in the organs of the treated animals. Tissue lysates from the organs of the treated mice were prepared and assayed to determine GAG levels. Significant elevation of GAG storage was found in the heart, lung, liver, spleen and kidney of the untreated MPS II animals when compared to wild-type littermates (Fig. 4B; $p < 0.01$). GAG contents were normalized in all of the tested peripheral organs of the IV infused rAAV9.hIDS animals and were comparable to those of the wild-type littermates (Fig. 4B; $p > 0.05$). Significantly increased levels of GAG were observed in all 12 portions of brain for the untreated MPS II group (Fig. 4C; $p < 0.05$). No significant elevation of GAG content was observed in the spinal cord among the three groups (Fig. 4C; $p > 0.05$). Surprisingly, despite the low levels of IDS found in the CNS, normalization of GAG content was observed in all portions of the brain (Fig. 4C; $p > 0.05$ compared to wild-type). These data demonstrate that IV-administration of rAAV9.hIDS led to effective global correction of GAG storage in MPS II mice, including the CNS.

3.4. Persistent levels of IDS in the CNS after IV administration of rAAV9-hIDS prevent the emergence of neurocognitive deficits in MPS II mice

At 6 months of age (16 weeks post treatment), wild-type, untreated MPS II, and IV-treated MPS II mice were evaluated in two neurocognitive tests, Barnes maze and fear conditioning, to determine the effect of the treatment. The Barnes maze is a test of spatial navigation and memory [36], while fear conditioning measures a recollected aversive response [37]. Here we employ these tests to model cognitive function in human MPS II.

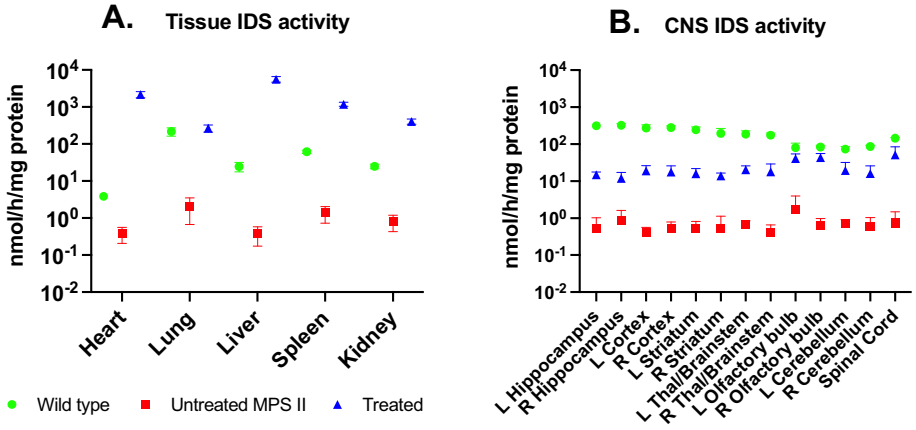

Fig. 2. Tissue IDS activities. Animals were sacrificed at end of study and organs were harvested and extracted for IDS assay. (A) Peripheral organs. 580-, 1.2-, 226-, 20- and 22-fold wild-type IDS activities were observed in the heart, lung, liver, spleen and kidney, respectively. (B) CNS tissues. Assay background levels of IDS activity were observed (<1.7 nmol/h/ml) in the untreated MPS II mice. In IV rAVV9.hIDS-treated animals, IDS activities at 4–26% of wild-type were observed in the 12 microdissected regions of the brain, except the olfactory bulb (51%) and the spinal cord (36%).

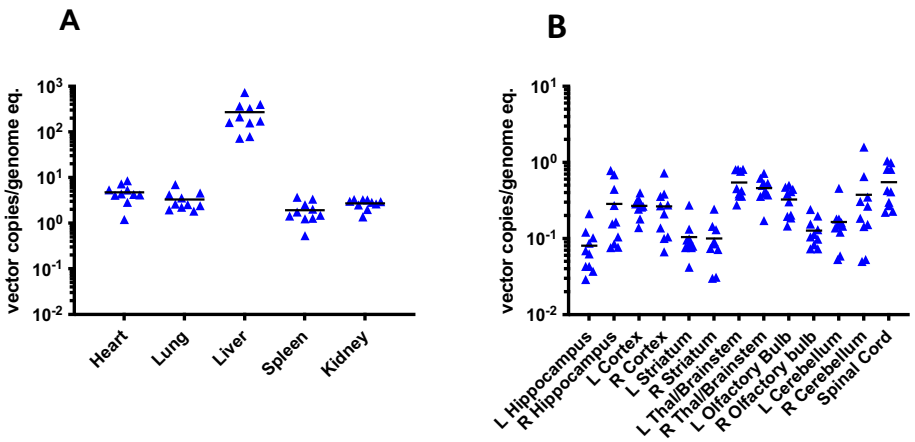

Fig. 3. rAAV9.hIDS vector biodistribution by quantitative PCR. Genomic DNA was extracted from the indicated tissues of rAAV9-hIDS treated mice and IDS vector sequences quantified by real-time quantitative PCR. (A) Peripheral organs. Biodistribution was observed in the heart, lung, liver, spleen, and kidney. The highest copy numbers were observed in the liver (mean 286 vg/ge), while low copy numbers (<5 vg/ge) were observed in the other peripheral organs. (B) CNS tissues. Relatively low copy numbers with an average of <1 vg/ge were detected in all of the 12 regions of the brain and the spinal cord.

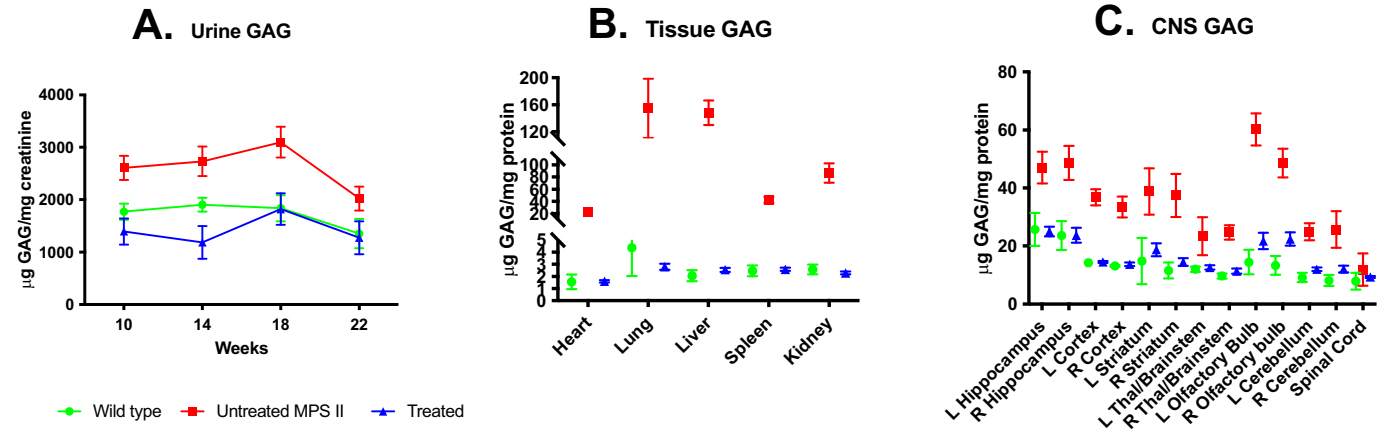

Fig. 4. Metabolic correction of GAG excretion and tissue storage disease. (A) Urine GAG was monitored from week 10 to 22 post injection. Elevated urine GAG was observed in untreated MPS II mice throughout the study. Normalization of urine GAG in the IV-treated mice was observed as early as 10 weeks post treatment and remained normalized throughout the study ($p > 0.05$ vs wild-type). (B) Peripheral tissues. The levels of tissue GAGs in the heart, lung, liver, spleen and kidney of the untreated MPS II animals were significantly higher than the IV-rAAV.hIDS-treated or the wild-type groups ($p < 0.01$). Normalization of peripheral tissue GAGs was observed in the IV-treated group ($p > 0.05$ vs wild-type). (C) CNS tissues. There was no significant difference in GAG content of the spinal cord among the three groups. Significant elevation of GAGs was observed in the 12 regions of the brain of the untreated MPS II mice compared to wt ($p < 0.05$) and compared to the IV-rAAV.hIDS treated group ($p < 0.05$). Normalization of GAG was observed in all 12 regions of the brain of the treated group ($p > 0.05$ vs wild-type).

Barnes Maze: All of the mice in the three groups were evaluated in the Barnes maze at 16 weeks post treatment. Wild-type mice showed reduced latency to escape over the course of 6-day trials from 165 s on day 1 down to 29 s on day 6. In contrast, the untreated MPS II mice showed improvement from 150 s to 80s between days 1 to 3, but no improvement in latency to escape from days 3–6 at 80s (Fig. 5A; $p < 0.05$ vs wt). Surprisingly, the treated MPS II mice showed remarkable spatial navigation and memory to escape the maze throughout the trials. Significant reduction in the latency to escape was observed on day 6, at 20s, markedly outperforming the untreated MPS II littermates on the same day (Fig. 5A; $p < 0.01$). We used ANOVA to determine whether or not there was a treatment x time interaction in the rate of learning (Fig. 5B) [34]. There was no significant treatment x time interaction (Fig. 5B; $p > 0.05$) between treated MPS II and wt mice, suggesting similar learning

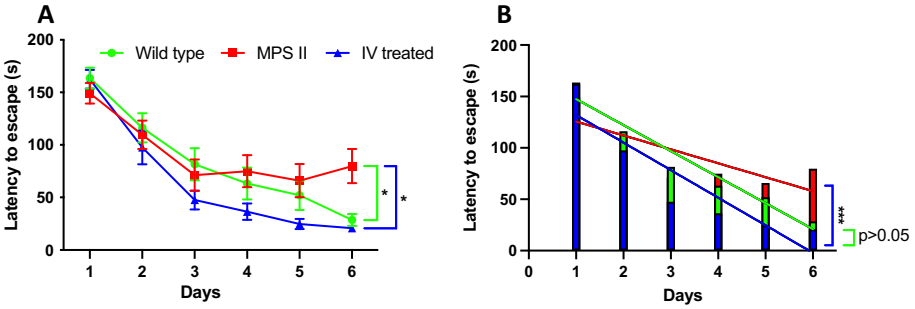

Fig. 5. IV rAAV-hIDS prevents neurocognitive dysfunction in the Barnes maze. Animals in all groups indicated were tested in the Barnes maze. (A) The average latency to escape (seconds) on each day of the trial is plotted for each group. The latency to escape for the wild-type and the IV-treated animals decreased over the course of 6 days. In contrast, the latency to escape for the untreated MPS II group showed no improvement from day 3 to day 6. The IV-treated animal performance was comparable to that of wild-type ($p > 0.05$), while the IV-treated animals outperformed the untreated MPS II mice on day 6 (*$p < 0.05$). (B) Learning slope (treatment x time interaction) analysis of the treated animals and wt littermates indicates no difference in learning rate ($p > 0.05$), while the treated group learned significantly faster than untreated MPS II littermates (***$p < 0.001$).

rates between these groups, while there was a significant treatment x time interaction (Fig. 5B; $p < 0.001$) between treated MPS II mice and untreated MPS II mice, indicating that treated MPS II mice learned at a faster rate than the untreated MPS II littermates. We observe that as low as 4% of wild-type IDS activity (Fig. 2B) was sufficient in the hippocampus to effectively prevent the emergence of spatial navigation and memory deficits in MPS II mice.

Fear conditioning assay: All groups of mice underwent fear conditioning the following week after testing in the Barnes maze. Fear test conditioning is used to measure learning memory of environmental cues that are associated with aversive experiences. The percentage freezing time during these trials is assessed as the fear memory response. There was no significant difference between the groups in percent freezing time during the first 3 min of the neutral environment without cues (Fig. 6 (1,2,3 on the x-axis); $p > 0.05$). However, when the aversive cues (light and sound without foot shock) were presented, wild-type littermates showed significantly increased percent freezing time during the second and the third minutes of the trial (94% and 95%, respectively) when compared to untreated MPS II littermates (Fig. 6, 72% and 68%, respectively (CS2, CS3 on the x-axis); $p < 0.01$). Importantly, the treated MPS II mice also showed significantly increased percent freezing time during the second (87%) and the third minutes (85%) when compared to the untreated MPS II littermates (Fig. 6, 72% and 68%, respectively; $p < 0.05$). No significant difference in percent freezing time was observed between wild-type and treated littermates (Fig. 6; $p > 0.05$). We conclude that IV administration of rAAV9.hIDS in MPS II mice at a young age prevented the loss of cognitive function. Overall, only 4% to 50% of the wild-type level of IDS activity in the brain was sufficient to protect against the emergence of neurocognitive deficits in the rAAV9.hIDS IV-treated animals.

4. Discussion

In this study, we demonstrated successful IV administration of AAV9 vector for hIDS gene transfer in C57BL/6 MPS II mice. hIDS cDNA was expressed using a strong CB7 promoter that led to previously unreported supraphysiological levels of IDS enzyme activity in the circulation, up to 9100 times that of wild type. Vector biodistribution indicated that in most of the tested tissues there was low level enzyme expression, while liver was the primary source of enzyme, supplying a large quantity of IDS to the system. In addition, we found that IV administration of rAVV9.hIDS led to high levels of IDS activity in all tested organs, ranging from 1.2- to 580-fold higher than wild-type. In this novel CNS biodistribution study, we report that IV rAAV9.hIDS resulted in the presence of IDS enzyme activity in all 12 portions of the micro-dissected brain, ranging from 4 to 50% that of wild-type. Furthermore, we observed that the sustained, high level of IDS activity in the circulation normalized urine GAG levels from the 10th week through the end of study. We also observed global normalization of GAGs in tested peripheral tissues and in the CNS. Finally, we observed that MPS II mice treated IV with rAAV9.hIDS at 2 months of age had the profound effect of preventing neurocognitive deficits, suggesting that as low as 4% to 50% of the wild-type enzyme level is sufficient to counteract the emergence of neurologic disease.

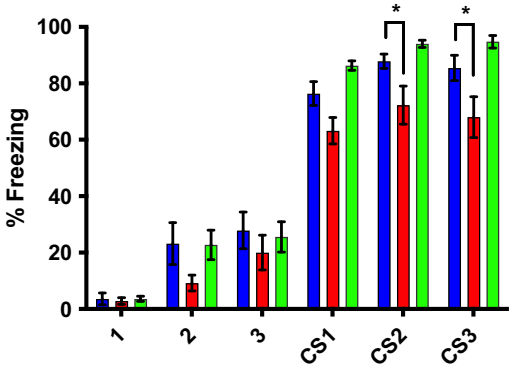

Fig. 6. IV rAAV-hIDS prevents neurocognitive dysfunction assessed by fear conditioning (cue test). No significant differences in % freezing time were observed during the first 3 min of acclimation (1–3) among three groups. When the aversive cue was presented for 3 min (CS1–3), significantly increased % freezing time was observed in the IV-treated mice during the 2nd and 3rd minute of the cue presentation (*$p < 0.05$ vs untreated MPS II).

The administration of rAAV9 vector to mediate gene transfer has been successfully evaluated in several preclinical models of lysosomal storage disorders [23,26,28,38], emphasizing its potential translation to clinical application. The nature of widespread viral tropism of rAAV9 and the ability to cross the blood brain barrier makes it an effective serotype for therapeutic gene transfer [29]. Previous studies have demonstrated that administration of AAV9 intracerebroventricularly (ICV) or intrathecally (IT) resulted in global viral distribution and global metabolic correction as well as an effective approach to prevent the emergence of neurocognitive deficits in MPS mouse models [17,26]. Herein our results suggest an alternative route of administration via non-invasive IV rAAV infusion that can potentially be as beneficial as ICV or IT for treating MPS II.

Intravenous administration of rAAV9.hIDS elicited a very robust response in MPS II mice, resulting in sustainable and high levels of IDS activity in the circulation that persisted for at least 22 weeks post-treatment (Fig. 1). We observed high levels of the enzyme in the heart, lung, liver, spleen and kidney (Fig. 2) at a low level of vector biodistribution to these organs, except the liver (Fig. 3A). These results implicate the liver as the primary site of rAAV9.hIDS transduction and the primary reservoir of enzyme expression. The resultant high level of IDS secreted into the circulation of the treated animals plays a critical role in metabolic cross-correction and delivery of enzyme for normalization of GAG storage in peripheral organs. This is consistent with our previous study of ICV administered MPS II mice, where we observed biodistribution of the rAAV9-hIDS vector in peripheral organs, indicating substantial vector release from the CSF into the circulation with subsequent transduction of peripheral tissues [17]. On the other hand, in this study we observed low level but definitive biodistribution of the rAAV9-hIDS in the CNS post IV administration (Fig. 3B), suggesting confirmation of rAAV9 penetrating the BBB. However, the low level of vector biodistribution in the CNS (Fig. 3B), indicates that the low level of IDS activity (Fig. 2B) observed could have come from one of two sources. First, it's possible that rAAV-hIDS transduced cells in the CNS were able to express and secrete a limited amount of IDS enzyme which then diffused for uptake into non-transduced CNS cells via the mannose-6 phosphate receptor. Second, it's possible that the presence of IDS enzyme in the CNS is caused by "high-dose effects" that have been reported in several MPS studies [20,39,40], whereby the consistent, high level of enzyme in the circulation results in passage of a fractional amount into the CNS. Alternatively, it is possible that the presence of IDS enzyme in the CNS resulted from a combination of both sources. However, it's also possible that the IDS activity assayed in brain tissue extracts was the result of high-level IDS present in the blood or in transduced endothelial cells of the blood vessels in the brain. All of the animals in our study were perfused with saline prior to organ harvest, eliminating the presence of IDS activity from contaminating blood. However, further investigation is needed to address the presence of IDS in or rAAV9-hIDS transduction of endothelial cells as the source of low-level IDS activity in brain extracts. Nonetheless, our data indicates that a minimum IDS activity of 4% to 50% of the wt level is required to prevent neurocognitive decline in the treated MPS II mice. Applicability of these results to humans must of course also consider the substantial size differential between mouse and human brain.

In conclusion, this study evaluates and emphasizes the benefits of intravascular (IV) administration as a non-invasive yet potentially effective procedure for rAAV9-hIDS delivery as genetic therapy for MPS

II. The most important finding in this study is that IV injection of the rAAV9 viral vector can have overall benefits on both sides of the BBB in mice: the peripheral organs and the CNS. Similar to our ICV study, IV administration resulted in global expression of the enzyme in all tested organs. The liver appears to be responsible for supplying a large portion of the enzyme that circulates and distributes enzyme globally throughout the system. Although IDS enzyme in the CNS was lower than expected, our results nonetheless provide further evidence that much <10% of the wild-type IDS level in the CNS is sufficient to bring significant neurologic benefits to the treatment in MPS II mice. Finally, our results emphasize and provide a non-invasive procedure that could potentially be effective in the treatment of MPS II. We anticipate that this study will encourage the field in developing IV AAV9 mediated gene transfer as an additional non-invasive avenue to treat human MPS II and other lysosomal storage disorders.

Data availability

Data will be made available on request.

Acknowledgements

The authors thank Dr. Joseph Muenzer for providing the IDS KO strain, and the University of Minnesota NINDS Behavioral Phenotyping Core. The work described in this manuscript was supported by REGENXBIO.

References

[1] E.F. Neufeld, J. Muenzer, The Mucopolysaccharidoses | The Online Metabolic and Molecular Bases of Inherited Disease | OMMBID | McGraw Hill Medical, McGraw-Hill Education, 2019 https://ommbid.mhmedical.com/content.aspx?sectionid=225544161&bookid=2709.
[2] I.V.D. Schwartz, et al., A clinical study of 77 patients with mucopolysaccharidosis type II, Acta Paediatr. 96 (2007) 63–70.
[3] J.E. Wraith, et al., Mucopolysaccharidosis type II (Hunter syndrome): a clinical review and recommendations for treatment in the era of enzyme replacement therapy, Eur. J. Pediatr. 167 (2008) 267–277.
[4] F.H. Bitencourt, et al., Medical costs related to enzyme replacement therapy for Mucopolysaccharidosis types I, II, and VI in Brazil: a multicenter study, Value Heal. Reg. Issues 8 (2015) 99–106.
[5] C. Lampe, et al., Long-term experience with enzyme replacement therapy (ERT) in MPS II patients with a severe phenotype: an international case series, J. Inherit. Metab. Dis. 37 (2014) 823–829.
[6] H. Sonoda, et al., A blood-brain-barrier-penetrating anti-human transferrin receptor antibody fusion protein for Neuronopathic Mucopolysaccharidosis II, Mol. Ther. 26 (2018) 1366–1374.
[7] T. Okuyama, et al., Iduronate-2-sulfatase with anti-human transferrin receptor antibody for neuropathic Mucopolysaccharidosis II: a phase 1/2 trial, Mol. Ther. 27 (2019) 456–464.
[8] C. Horgan, et al., Current and future treatment of Mucopolysaccharidosis (MPS) type II: is brain-targeted stem cell gene therapy the solution for this devastating disorder? Int. J. Mol. Sci. 23 (2022).
[9] A.L. Barth, et al., Early hematopoietic stem cell transplantation in a patient with severe mucopolysaccharidosis II: a 7 years follow-up, Mol. Genet. Metab. Rep. 12 (2017) 62–68.
[10] M.D. Poe, et al., Early treatment is associated with improved cognition in Hurler syndrome, Ann. Neurol. 76 (2014) 747–753.
[11] A. Selvanathan, et al., Effectiveness of early hematopoietic stem cell transplantation in preventing neurocognitive decline in mucopolysaccharidosis type ii: A case series, in: JIMD Reports vol. 41, Springer, 2018, pp. 81–89.
[12] T. Wakabayashi, et al., Hematopoietic stem cell gene therapy corrects neuropathic phenotype in murine model of Mucopolysaccharidosis type II, Hum. Gene Ther. 26 (2015) 357–366.
[13] M.C. Smith, et al., Phenotypic correction of murine mucopolysaccharidosis type II by engraftment of ex vivo lentiviral vector transduced hematopoietic stem and progenitor cells, Hum. Gene Ther. 33 (2022) 1279–1292.
[14] H. Fe Gleitz, et al., Brain-targeted stem cell gene therapy corrects mucopolysaccharidosis type II via multiple mechanisms, EMBO Mol. Med. 10 (2018), e8730.
[15] S. Miwa, et al., Efficient engraftment of genetically modified cells is necessary to ameliorate central nervous system involvement of murine model of mucopolysaccharidosis type II by hematopoietic stem cell targeted gene therapy, Mol. Genet. Metab. 130 (2020) 262–273.
[16] M. Cardone, et al., Correction of hunter syndrome in the MPSII mouse model by AAV2/8-mediated gene delivery, Hum. Mol. Genet. 15 (2006) 1225–1236.
[17] K. Laoharawee, et al., Prevention of neurocognitive deficiency in mucopolysaccharidosis type II mice by central nervous system-directed, AAV9-mediated iduronate sulfatase gene transfer, Hum. Gene Ther. 28 (2017).
[18] H. Fu, et al., Targeting root cause by systemic scAAV9-hIDS gene delivery: functional correction and reversal of severe MPS II in mice, Mol. Ther. Methods Clin. Dev. 10 (2018) 327–340.
[19] RGX-121 Gene Therapy in Patients With MPS II (Hunter Syndrome) - Full Text View. http://ClinicalTrials.gov", 2022. https://clinicaltrials.gov/ct2/show/NCT03566043.
[20] K. Laoharawee, et al., Dose-dependent prevention of metabolic and neurologic disease in murine MPS II by ZFN-mediated in vivo genome editing, Mol. Ther. 26 (2018).
[21] F. Huda, et al., Distinct transduction profiles in the CNS via three injection routes of AAV9 and the application to generation of a neurodegenerative mouse model, Mol. Ther. Methods Clin. Dev. 1 (2014) 14032.
[22] J.J. Glascock, et al., Delivery of therapeutic agents through intracerebroventricular (ICV) and intravenous (IV) injection in mice, J. Vis. Exp. 2–5 (2011), https://doi.org/10.3791/2968.
[23] V. Haurigot, et al., Whole body correction of mucopolysaccharidosis IIIA by intracerebrospinal fluid gene therapy, J. Clin. Invest. 123 (2013) 3254.
[24] K. Laoharawee, et al., Prevention of Neurocognitive Deficiency in Mucopolysaccharidosis Type II Mice by Central Nervous System–Directed, AAV9-Mediated Iduronate Sulfatase Gene Transfer, Hum. Gene Ther. 28 (2017) 626–638.
[25] D.A. Wolf, et al., Direct gene transfer to the CNS prevents emergence of neurologic disease in a murine model of mucopolysaccharidosis type I, Neurobiol. Dis. 43 (2011) 123–133.
[26] L.R. Belur, et al., High level expression of human Iduronidase throughout the brain in a murine model of Mucopolysaccharidosis type I after NonInvasive AAV-mediated gene delivery to the CNS, Mol. Ther. 22 (2014) S236.
[27] C. Weismann, et al., Systemic AAV9 gene transfer in adult GM1 gangliosidosis mice reduces lysosomal storage in CNS and extends lifespan, Hum. Mol. Genet. 24 (2015) 4353–4364.
[28] H. Fu, et al., Correction of neurological disease of mucopolysaccharidosis IIIB in adult mice by rAAV9 trans-blood-brain barrier gene delivery, Mol. Ther. 19 (2011) 1025–1033.
[29] J.R. McLean, et al., Widespread neuron-specific transgene expression in brain and spinal cord following synapsin promoter-driven AAV9 neonatal intracerebroventricular injection, Neurosci. Lett. 576 (2014) 73–78.
[30] D.J. Schuster, et al., Biodistribution of adeno-associated virus serotype 9 (AAV9) vector after intrathecal and intravenous delivery in mouse, Front. Neuroanat. 8 (2014) 42.
[31] C.N. Mattar, et al., Systemic gene delivery following intravenous administration of AAV9 to fetal and neonatal mice and late-gestation nonhuman primates, FASEB J. 29 (2015) 3876–3888.
[32] F.E. Harrison, et al., Spatial and nonspatial escape strategies in the Barnes maze, Learn. Mem. 13 (2006) 809–819.
[33] M. Martin-Fernandez, et al., Synapse-specific astrocyte gating of amygdala-related behavior, Nat. Neurosci. 20 (2017) 1540–1548.
[34] S.L. Inman-Wood, et al., Effects of prenatal cocaine on Morris and Barnes maze tests of spatial learning and memory in the offspring of C57BL/6J mice, Neurotoxicol. Teratol. 22 (2000) 547–557.
[35] L. López-Marín, et al., Detection by urinary gag testing of mucopolysaccharidosis type ii in an at-risk spanish population, in: JIMD Reports vol. 10, Springer, 2013, pp. 61–68.
[36] P.N. Pompl, et al., Adaptation of the circular platform spatial memory task for mice: use in detecting cognitive impairment in the APPSW transgenic mouse model for Alzheimer's disease, J. Neurosci. Methods 87 (1999) 87–95.
[37] R.G. Phillips, et al., Differential contribution of amygdala and hippocampus to cued and contextual fear conditioning, Behav. Neurosci. 106 (1992) 274–285.
[38] M.R. Haddad, et al., Fetal brain-directed AAV gene therapy results in rapid, robust, and persistent transduction of mouse choroid plexus epithelia, Mol. Ther. Nucl. Acids 2 (2013), e101.
[39] L. Ou, et al., A highly efficacious PS gene editing system corrects metabolic and neurological complications of Mucopolysaccharidosis type I, Mol. Ther. 28 (2020) 1442–1454.
[40] L. Ou, et al., High-dose enzyme replacement therapy in murine hurler syndrome, Mol. Genet. Metab. 111 (2014) 116–122.